Double arrow shaped negative index metamaterial for tri-band applications

SIKDER SUNBEAM ISLAM[a,b], MD. MEHEDI HASAN[a], MOHAMMAD RASHED IQBAL FARUQUE[a], MOHAMMAD TARIQUL ISLAM[c]
[a]*Space Science Centre (ANGKASA), Universiti Kebangsaan Malaysia, Bangi 43600, Malaysia*
[b]*Department of EEE, International Islamic University Chittagong, Chittagong, Bangladesh*
[c]*Department of Electrical, Electronic and Systems Engineering, Universiti Kebangsaan Malaysia, Bangi 43600, Malaysia*

A double-arrow-shaped negative refractive index (NRI) metamaterial is presented that magnetic inclusion was etched by copper over the epoxy resin composite with woven glass fabric, and its performance was investigated for two incidences (x- and z-axis) of the metamaterial. The numerical and experimental transmittance (S_{21}) are well compiled at 6.52 GHz, whereas the metamaterial shows double negative characteristics at 7.51 GHz. Further, the NRI metamaterial refractive index curve shows the negative region peaks from 5.01 GHz to 6.06 GHz (nearly 1 GHz bandwidth) and 7.37 GHz to 10 GHz (more than 2 GHz bandwidth) in the microwave regions for the z-axis wave propagation. A circuit model and necessary experimental results were provided to demonstrate the resonant behavior. Besides, the metamaterial displays the NRI property in the region of S-, C- and X-bands for the x-axis transmission with better effective medium properties.

1. Introduction

Metamaterial is an artificially engineered composite material that exhibits some exotic electromagnetic properties and overcomes the usual limitations of natural available materials. These extraordinary properties of metamaterial may include negative permittivity, negative permeability, inverted Snell's law and some other similar reverse electromagnetic phenomena. Through proper tailoring of effective medium properties (including permittivity, permeability, and refractive index) of metamaterial, electromagnetic waves can be controlled easily. For a certain electromagnetic application in the specific range of frequency, the size of the metamaterial unit cell should be much smaller than the target wavelength of operation. After the first successful invention of metamaterial by Smith and his colleagues [1], it has been utilized in almost all applications of electromagnetism due to its exciting electromagnetic properties. The applications of metamaterials have been explored in the field of designing antennas [2-4], designing filters, electromagnetic absorption, invisible cloaking [5] and increasing the efficiency of solar cells. However, the negative refractive index (NRI) property has been one of the most important properties of metamaterial in recent applied physics research. Metamaterials are usually designed adopting different dielectric materials. Dielectric materials with a higher dielectric constant enhance the capability of charge storage and provide larger fields, enabling limited conductor isolation. In contrast, a lower dielectric constant exhibits good insulation for the lower-order signals that need increased separation in

compact circuits [6]. Therefore, dielectric materials with improved performance that may reduce size, weight and cost, providing manufacturing ease for composite structures, are utilized for most metamaterial construction. The woven glass fabric with epoxy resin (FR-4) composite is such a type of material that has become popular in many applications. To design a metamaterial, the unit cell is first designed on a dielectric material. After that, its performance is investigated, and then the bulk metamaterial is prepared using the unit cells. However, the bulk metamaterial displays the same performance as the unit cell.

Numerous metamaterial structures were proposed in the literature, but few of them are suitable for two-component operation with the NRI property. A single layer negative index meta atom was described, which was developed by an outer and inner split ring resonators with inverse E-shape metal strips of copper are connected with the outer ring resonator that look like a mirror-shape structure. This design illustrated 5.81 GHz wide bandwidth and applicable for tri (C-, X- and Ku-) band application. The total dimensions of the designed structure were $0.2\lambda \times 0.2\lambda \times 0.035\lambda$ and the effective medium ratio was 5 [7]. S.S. Islam et al. proposed an S-band metamaterial in [8], but their metamaterial showed neither NRI properties nor two-component operation. Another multiband metamaterial was claimed in [9] in the microwave range with NRI properties but was not proved for two-component operation. In [10], a DNG metamaterial structure presented that combination of the splits and square S-shape ring resonators. The proposed unit cell exhibits resonances at X-band with negative

refractive index from 8.0 to 11.70 GHz and 11.78 to 14.0 GHz, i.e. the bandwidths cover 3.70 GHz and 2.22 GHz, respectively with negative index characteristics in 11.92 GHz. In [11] a negative index metamaterial with two components analysis for C- and X-band had been introduced by Islam et *al*. and the structure had two arrows and a metal arm was connected the two arrows that looked like a double arrow shape printed on the epoxy resin fibre and the epoxy resin formation processes were also explained step by step in 2017. Hasan et *al*. [12], proposed a compact double-negative metamaterial for wideband operations. This metamaterial structure was applicable for S-, C- and X-band applications but was not analyzed for two-component operation. In this study, we are proposing a new double-arrow-shaped metamaterial unit cell structure for two-component multiband operation with the NRI property. The metamaterial was designed on epoxy resin composite. Commercial electromagnetic software application CST Microwave studio was used for the analysis of the metamaterial properties.

2. Construction of the Unit Cell

Fig. 1 (a) delineates the proposed NRI metamaterial unit cell. For the experimental verification, the fabrication of the unit cell was performed. The fabricated unit cell is shown in the Figure-1 (b). The proposed unit cell specifications are shown in Table 1.
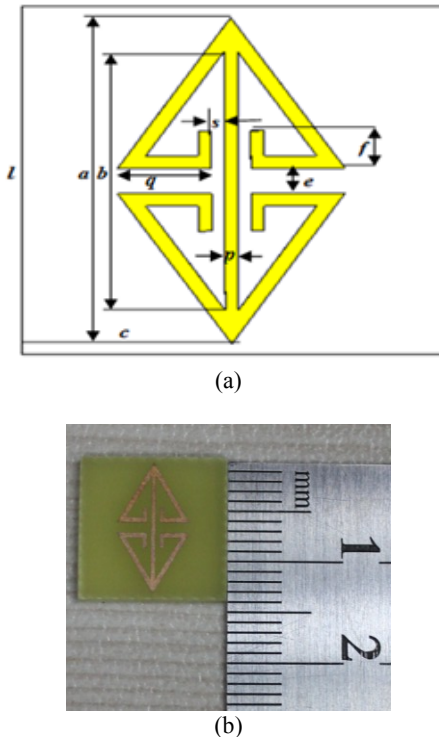

(a)

(b)

*Fig. 1. Proposed metamaterial single unit cell:
(a) Schematic structure, (b) Fabricated structure*

Two metal (copper) arms were coincided at a 45-degree angle to make an arrow-type shape. Two arrows were framed facing opposite directions and were connected by a metal stripe to construct a double-arrow-shaped structure. The copper thickness was kept at 0.035 mm over the entire design. The unit cell was printed over the 14×14 mm^2 epoxy resin with woven glass fabric composite. The composite has a complex dielectric constant ε_c= 4.3+j 0.025 and thickness of 1.6 mm. The design parameters for the unit cell are presented in Table 1.

Table 1. Designed parameters of the presented unit cell.

Para.	a	b	c	e	f	s	l	p	q
Size	13	10	7.0	1.0	1.5	0.5	14	0.5	3.0

3. Methodology

In this paper, dielectric material epoxy resin with woven glass fabric composite was used as a substrate material. In this study, the microwave simulation tool CST Microwave Studio was chosen to calculate the S-parameters. The unit cell was set in a manner that electromagnetic waves go along the Z-axis, and two waveguide ports were used. The boundary condition, a perfect electric–magnetic conductor, was adopted for the simulation, where a perfect electric field was applied in the x-axis and a perfect magnetic field in the y-axis. Simulation was performed over the frequency range of 1.0 to 10 GHz. The technique specified in [13] was utilized to calculate the permittivity, permeability, and refractive index of the material from the estimation of S_{21} and S_{11}. For double-negative features, inductance and capacitance are formed in the proposed unit cell equivalent circuit by the series and shunt branch of the inductor and capacitor shown in Figure-2. In the circuit, the gaps created capacitance symbolized by C1 and C2 in the circuit. Conversely, the metal strips created inductance represented by L1, L2, L3, L4 and L5. By increasing the width of the metal strips, the inductive effect can be increased, resulting in decreased resonance frequency. Similarly, by increasing the number of gaps, the capacitive effect can be raised, and the resonance is declined in the frequency band. Due to the addition of more metal strips, the total inductive effect increased in the designed unit cell structure, and it exhibited resonance at 6.52 GHz.
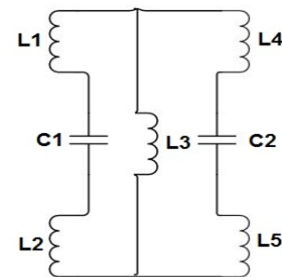

Fig. 2. Equivalent LC circuit of the metamaterial single unit cell.

As this type of metamaterial contains passive LC-circuits, the resonance frequency would be,

$$f = \frac{1}{2\pi\sqrt{LC}} \qquad (1)$$

where C and L are the total capacitance and inductance, respectively, of the structure. Usually, in relation to the quasi-static theory, the total capacitance formed between gaps is

$$C = \varepsilon_0\varepsilon_r \frac{A}{d}(F) \qquad (2)$$

where ε_0 and ε_r are the permittivity of free space and the relative permittivity, respectively; "A" is the cross-sectional area of the gap; and "d" is the gap length. However, the inductance of the proposed structure can be expressed as,

$$L \approx 2\mu_0 t \left\{ \left(\frac{\sqrt{f-e}}{2(a+b)^2} \right) - \left(\frac{\sqrt{c-2q-s}}{4(a^2+b^2)} \right) \right\} \qquad (3)$$

And the capacitance can be written as,

$$C \approx \varepsilon_0 \left\{ \left(\frac{2(q+s)}{\pi} \right) \ln \left(\frac{l-a}{p} \right) \right\} \qquad (4)$$

where the free space permeability is $\mu_0 = 4\pi \times 10^{-7}$ H/m and the permittivity is $\varepsilon_0 = 8.85 \times 10^{-12}$ F/m. A more detailed discussion of the above equations can be found in the literature [14] and [15]. Two C-band (WR137) waveguides were used as a transmitter and receiver, and the fabricated unit cell was placed between them. The waveguides were linked to the network analyzer named 'Agilent E8363D' to find the S-parameters. For alignment reasons, estimation without metamaterial and with metamaterial was performed.

4. Results and discussions

The current distribution for the unit cell at 6.52 GHz is shown in Fig. 3(a) where current flowing is seen in the two opposite side arrows of the unit cell. This flow of opposite current results a sharp transmittance at that frequency. In Figure-3(b), the numerical and experimental transmission parameter (S_{21}) for the double-arrow-shaped unit cell is shown. It demonstrates that the extent of S_{21} displays a resonance at 6.52 GHz. According to the circuit model of the proposed metamaterial unit cell, the calculated resonance frequency is 6.47 GHz, which is very close to the simulated value. However, the experimental transmission property of the metamaterial for the unit cell is also presented in the same figure for the comparison. The measured result shows good conformity with the simulated result.
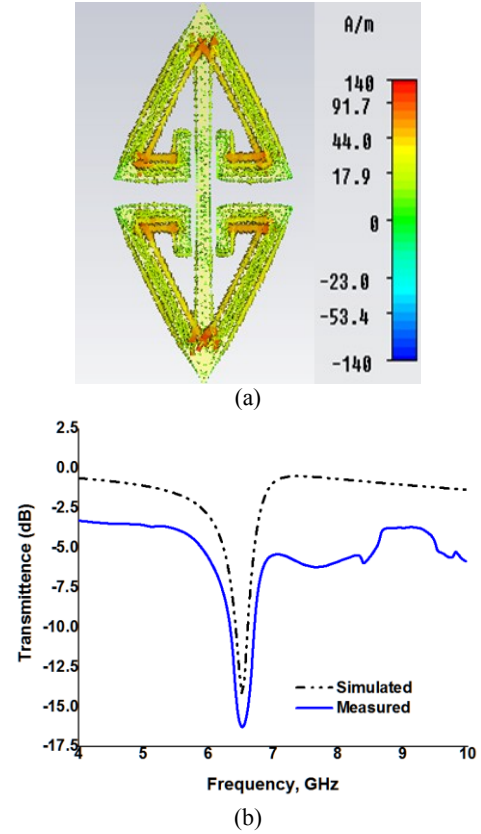

(a)

(b)

Fig. 3. (a) Current distribution at 6.52 GHz, (b) Magnitude of simulated and measured transmission of the unit cell.
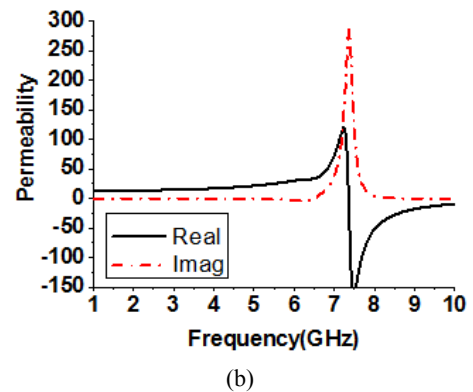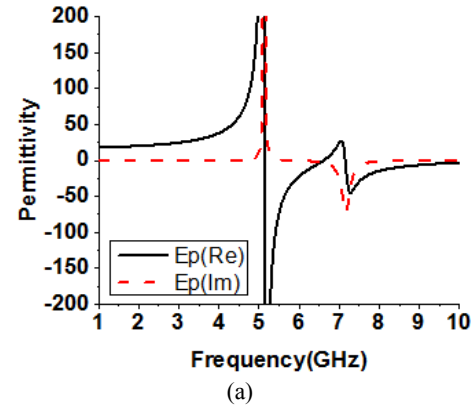

(a)

(b)

Fig. 4. Effective: (a) permittivity, (b) permeability, against frequency for z-axis wave propagation.

The figured permittivity (ε) in addition to permeability (μ) against frequency is depicted in Fig. 4(a) and Fig. 4(b). In Fig. 4(a), the real magnitude of the permittivity displays a negative value from 5.16 GHz to 6.62 GHz and 7.18 GHz to 10 GHz, which covers a nearly 3 GHz bandwidth. At 6.52 GHz, ε= -3.58-j2.15. Fig. 4(b) depicts the permeability of the material where the curve displays the negative peak from 7.37 GHz to 10 GHz, which covers more than a 2 GHz bandwidth in the microwave regime.
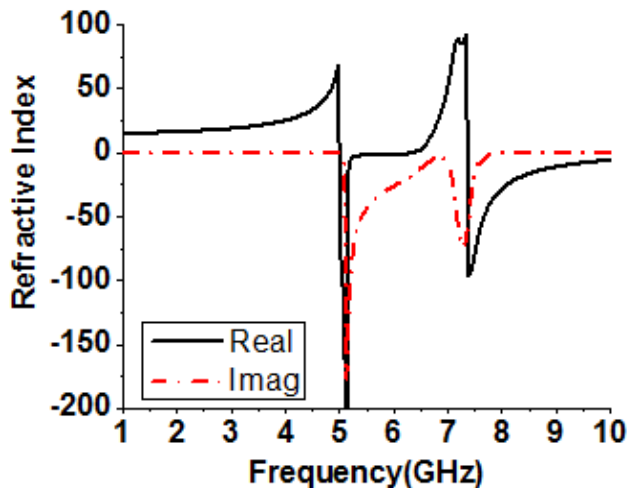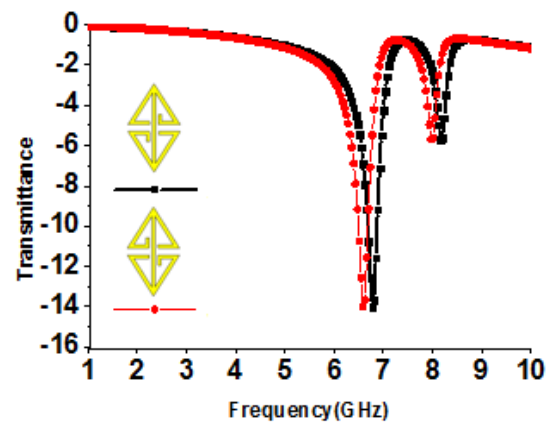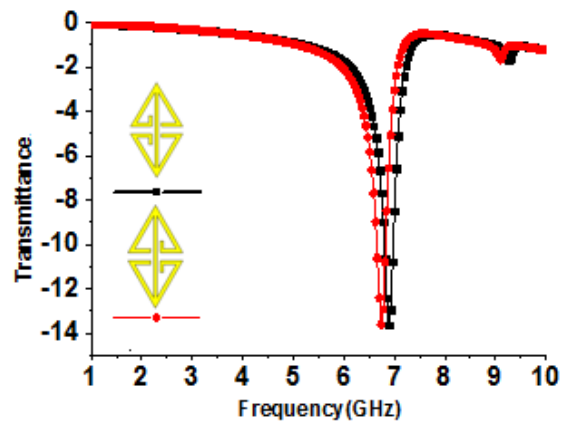

Fig. 5. Refractive index (n) curve for unit cell in the z-axis

Fig. 5 describes the refractive index (η) curve against frequency for the z-axis wave propagation through the unit cell. It is evident from the curve that the negative region peaks from 5.01 GHz to 6.06 GHz (nearly 1 GHz bandwidth) and 7.37 GHz to 10 GHz (more than 2 GHz bandwidth). The first bandwidth of the negative peak falls in the C-band, and the second bandwidth falls in the X-band. The first bandwidth of the negative peak of the refractive index has occurred due to the chiral effect. Moreover, in these negative zones of the refractive index curve, the permeability and permittivity curve also displays a negative peak. This is why the material can be characterized as a double-negative (DNG) metamaterial in these regions of microwave spectra. Further analysis was performed with the metamaterial unit cell for the x-axis wave flowing through the unit cell of the metamaterial. For that, the waveguide ports were set at the two sides of the material unit cell along the x-axis, and the same simulation setup was considered.
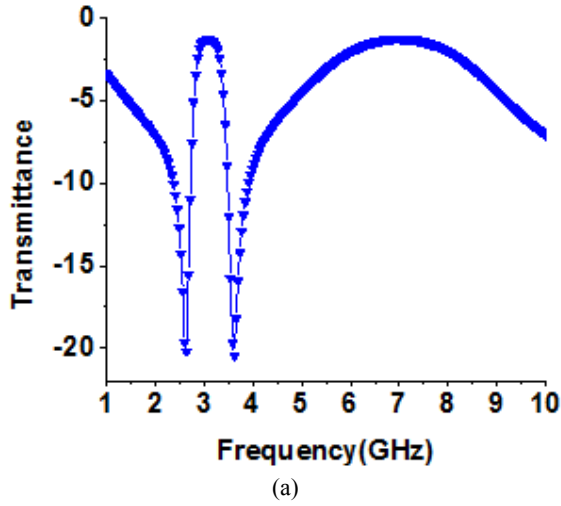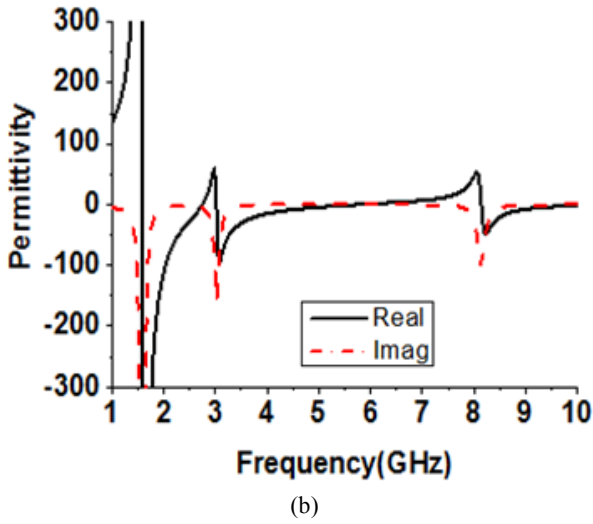

(a)

(b)

Fig. 6. Modification effect of, (a) Opposite arms, (b) Same-side arms of the designed structure on transmittance (S_{21})

Fig. 6(a) displays the transmittance caused by the modified arms at two opposite sides of the unit cell for z-axis wave flow. The considerable resonance is seen at the frequency of 6.60 GHz for the modification at upper-left and down-right side of the unit cell and for the modification at down-left and upper-right side of the unit cell, the resonance is found almost at same position at 6.67 GHz. In Figure-6(b), the transmittance caused by the modified arms at the same side of the unit cell is presented due to z-axis wave propagation. One sharp resonance is found at the frequency of 6.73 GHz for the modification at up-down right side and at 6.80 GHz (which is very close to 6.73 GHz) for the modification at up-down left side of the unit cell. However, for the proposed unit cell (in Figure-1(b)) shows resonance at 6.52 GHz which has formed due to different polarization for the combination of both side modifications.
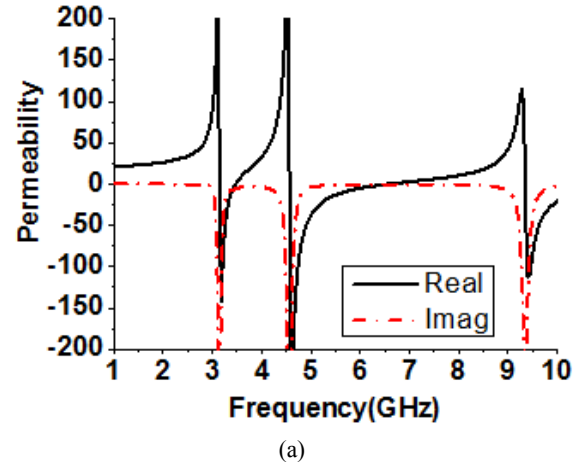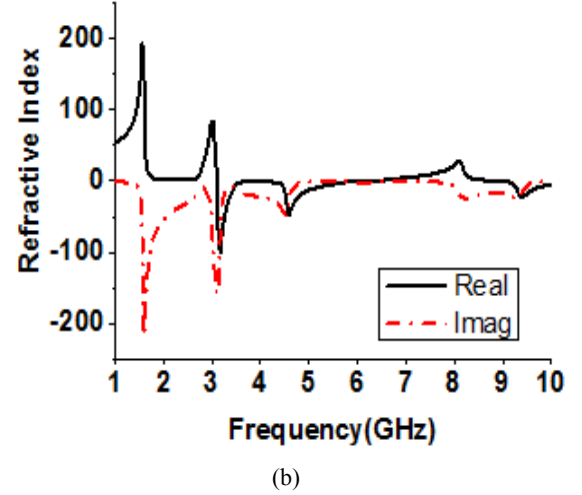
(a)

(b)

Fig. 7. Magnitude of: (a) transmission coefficient, (b) effective permittivity (ε) due to x-axis wave propagation.

(a)

(b)

Fig. 8. Effective: (a) permeability (μ), (b) refractive index (n) against frequency due to x-axis wave propagation.

Fig. 7(a) displays the simulated transmission property for the unit cell of metamaterial due to x-axis wave propagation through the unit cell. Two transmittances are found in the microwave range at the frequencies of 2.65 GHz and 3.62 GHz. In Figure-7(b), the curve of effective permittivity is shown for the x-axis wave propagation through the unit cell. The permittivity curve shows a negative peak from 1.6 GHz to 2.70 GHz with more than 1 GHz bandwidth, 3.02 GHz to 5.76 GHz with more than 2 GHz bandwidth and 8.16 GHz to 10 GHz with more than 1.5 GHz bandwidth. However, at 2.65 GHz and 3.62 GHz, the permittivity curve displays a negative magnitude as well with ε = -12.69-j3.50 and ε = -25.22-j1.18, respectively.

Fig. 8(a) reveals the effective permeability curve for the unit cell due to x-axis wave propagation. The permeability curve displays a negative magnitude from 3.17 GHz to 3.43 GHz, 4.62 GHz to 6.55 GHz (which covers more than 2 GHz bandwidth) and 9.36 to 10 GHz. Figure-8(b) shows the refractive index curve for the unit cell due to x-axis wave propagation.

The refractive index graph displays the negative peak from 3.17 GHz to 4 GHz that covers more than 700 MHz bandwidth, 4.15 GHz to 6 GHz that includes more than 1.5 GHz bandwidth, and 8.90 GHz to 10 GHz that also contains more than 1 GHz bandwidth. Therefore, these negative zones are considered as NRI regions. Among these negative zones, the first zone falls in the S-band, the second zone in the C-band and the third zone in the X-band. However, within these negative zones, double-negative (DNG) regions (where both permittivity and permeability are negative with a negative refractive index property) are found from 3.17 GHz to 3.43 GHz, 4.62 GHz to 5.76 GHz and 9.36 GHz to 10 GHz. Therefore, these areas are regarded as DNG regions of the metamaterial. However, all negative frequency ranges are within the area of the S-, C- and X-bands of the microwave regime. Moreover, at 2.65 GHz, the refractive index curve displays a positive magnitude value n= 2.82-j22.35, and at 3.62 GHz, the refractive index curve displays a negative magnitude with n = -1.73-j17.36.

5. Conclusion

This paper explains a new metamaterial with a multiband NRI property for two-component operation. The dielectric material epoxy resin (FR-4) with woven glass fabric composite was used as substrate material to construct the metamaterial. The metamaterial also displays a DNG property in the multiband region. For the z-axis wave propagation, the material shows the NRI property in the C- and X-bands, but for the x-axis wave flow, the material exhibits NRI characteristics in the S-, C- and X-band regions of the microwave spectrum. However, the C-band of the microwave field is often utilized for remote correspondence. S- and X-bands are well known for satellite communications. Therefore, the proposed metamaterial will be a potential option for electromagnetic applications in these ranges.

References

[1] D. R. Smith, J. W. Padilla, D. C. Vier, S. C. Nemat-Nasser, S. Schultz, Physical Review Letters **84**, 4184 (2000).

[2] R. Azim, M. T. Islam, N. Misran, Journal of Infrared, Millimeter, Terahertz Waves **38**, 969 (2010).

[3] R. Azim, M. T. Islam, N. Misran, IEEE Antennas and Wireless Propagation Letters **10**, 1190 (2011).

[4] M. M. Islam, M. T. Islam, M. Samsuzzaman, M. R. I. Faruque, N. Misran, M. F. Mansor, Materials **8**, 392 (2015).

[5] S. S. Islam, M. R. I. Faruque, M. T. Islam, Scientific Reports **6**, Article number: 33624 (2016).

[6] S. A. Aguayo, Antenna Systems and Technology **12**, 14 (2010).

[7] M. M. Hasan, M. R. I. Faruque, M. T. Islam, IEEE Access **5**, 21217 (2017).

[8] S. S. Islam, M. R. I. Faruque, M. T. Islam, Journal of Electrical and Electronics Engineering **7**(2), 13 (2014).

[9] S. S. Islam, M. R. I. Faruque, M. T. Islam, Materials **7**, 4994 (2014).

[10] M. M. Hasan, M. R. I. Faruque, M. T. Islam, Bulletin of the Polish Academy of Sciences Technical Sciences **65**, 533 (217).

[11] S. S. Islam, M. M. Hasan, M. R. I. Faruque, M. M. Islam, M. T. Islam, Microwave and Optical Technology Letters **59**, 1092 (2017).

[12] M. M. Hasan, M. R. I. Faruque, M. T. Islam, Applied Sciences **7**, 1071 (2017).

[13] O. Luukkonen, S. I. Maslovski, S. A. Tretyakov, IEEE Antennas and Wireless Propagation Letters **10**, 3588 (2011).

[14] R. P. Clayton, Inductance: Loop and Partial; Wiley-IEEE Press: Hoboken, NJ, USA, 2009.

[15] M. M. Hasan, M. R. I. Faruque, M. T. Islam, Materials Research Express **4**, 035015 (2017).

_____
[*]Corresponding author: sikder_islam@yahoo.co.uk, mehedi.hasan.ukm@gmail.com, rashed@ukm.edu.my, tariqul@ukm.edu.my